Nuclear Engineering and Technology xxx (xxxx) xxx

Contents lists available at ScienceDirect

Nuclear Engineering and Technology

journal homepage: www.elsevier.com/locate/net

Effect of mitigation strategies in the severe accident uncertainty analysis of the OPR1000 short-term station blackout accident

Wonjun Choi [a], Kwang-Il Ahn [b], Sung Joong Kim [a, c, *]

[a] Department of Nuclear Engineering, Hanyang University, 222 Wangsimni-ro, Seongdong-gu, Seoul, 04763, Republic of Korea
[b] Korea Atomic Energy Research Institute, 989-111 Daedeok-daero, Yuseong-gu, Daejeon, 34057, Republic of Korea
[c] Institute of Nano Science & Technology, Hanyang University, 222 Wangsimni-ro, Seongdong-gu, Seoul, 04763, Republic of Korea

ARTICLE INFO

Article history:
Received 25 February 2022
Received in revised form
17 June 2022
Accepted 31 July 2022
Available online xxx

Keywords:
OPR1000
Severe accident
Short-term station blackout
Severe accident mitigation
Uncertainty and sensitivity analysis

ABSTRACT

Integrated severe accident codes should be capable of simulating not only specific physical phenomena but also entire plant behaviors, and in a sufficiently fast time. However, significant uncertainty may exist owing to the numerous parametric models and interactions among the various phenomena. The primary objectives of this study are to present best-practice uncertainty and sensitivity analysis results regarding the evolutions of severe accidents (SAs) and fission product source terms and to determine the effects of mitigation measures on them, as expected during a short-term station blackout (STSBO) of a reference pressurized water reactor (optimized power reactor (OPR)1000). Three reference scenarios related to the STSBO accident are considered: one base and two mitigation scenarios, and the impacts of dedicated severe accident mitigation (SAM) actions on the results of interest are analyzed (such as flammable gas generation). The uncertainties are quantified based on a random set of Monte Carlo samples per case scenario. The relative importance values of the uncertain input parameters to the results of interest are quantitatively evaluated through a relevant sensitivity/importance analysis.

1. Introduction

During a severe accident (SA), various physical and chemical phenomena occur simultaneously and interact with one another. Representative SA phenomena include the oxidation of the Zircaloy (Zr) cladding, cooling of the molten corium, creep ruptures of reactor coolant system (RCS) pressure boundaries such as the coolant pipe or reactor pressure vessel (RPV), molten corium concrete interactions (MCCIs), and the release, transport, and sedimentation of fission products (FPs). These phenomena have been studied in experimental and numerical research studies, with the goal of predicting the progress of SAs based on computer codes [1–8]. Nevertheless, it remains difficult to predict the progress of SAs, owing to the many uncertainties existing in predicting SA phenomena. The uncertainties can step from a lack of knowledge, complex phenomenological interactions, and/or harsh experimental conditions. For example, the core degradation is observed at high temperature near 2,500 K ~3,000 K. In addition, various phenomena such as the oxidation of zircaloy, release of fission product, candling of molten corium, the radiative heat transfer and embrittlement of core geometry simultaneously occur during core degradation. Therefore, it is difficult to perform the pin-point experiment to cover the complex interaction and harsh conditions. This leads to the incomplete knowledge for the physical mechanism to predict the phenomenon, which causes the uncertainties.

A variety of studies have been performed aiming to understand the uncertainties addressed in SA code analysis, mainly focusing on the ranges of relevant uncertainties and importance (or sensitivity) of input parameters [9–12]. For example, the U.S. Nuclear Regulatory Commission performed uncertainty analyses to investigate the radiological consequences of pressurized water reactors (PWRs) and boiling water reactors, under the umbrella of the "State-of-the-Art Reactor Consequence Analyses" (SOARCA) project [13]. Through the SOARCA project, the uncertainties and major contributors to the source terms, especially the release fraction of Cs and I, were investigated while considering unmitigated short- and long-term station blackout (SBO) accidents using Monte Carlo sampling and regression-based sensitivity/importance analyses [11,14]. Besides, a few additional studies have been conducted aiming to quantify the

* Corresponding author. Department of Nuclear Engineering, Hanyang University, 222 Wangsimni-ro, Seongdong-gu, Seoul, 04763, Republic of Korea.
E-mail address: sungjkim@hanyang.ac.kr (S.J. Kim).

https://doi.org/10.1016/j.net.2022.07.029

Abbreviation

Cs	Cesium
CV	Control Volume
DAKOTA	Design Analysis Kit for Optimization and Terascale Applications
EWI	External Water Injection
FP	Fission Product
LH	Lower Head
LHS	Latin Hypercube Sampling
MCCI	Molten Corium Concrete Reaction
OPR1000	Optimized Power Reactor 1000 MWe
PRCC	Partial Ranked Correlation Coefficient
PWR	Pressurized Water Reactor
QUASAR	Quantification and Uncertainty Analysis of Source terms for severe
RCS	Reactor Coolant System
RCP	Reactor Coolant Pump
RPV	Reactor Pressure Vessel
SA	Severe Accident
SAG	Severe Accident Guideline
SAM	Severe Accident Management/Mitigation
SAMG	Severe Accident Management Guidance
SBO	Station Blackout
SDS	Safety Depressurization System
SNAP	Symbolic Nuclear Analysis Package
SRRC	Standardized Ranked Regression Coefficient
STSBO	Short-Term Station Blackout
Zr	Zircaloy

uncertainty in SA codes, focusing on in-vessel and ex-vessel hydrogen generation [15], core degradation [16], characteristics of the molten corium after vessel failure [17], and MCCIs [12]. Most previous studies adopted an approach based on the "Quantification and Uncertainty Analysis of Source Terms for Severe Accidents in Light Water Reactors" (QUASAR) methodology [18]. For reference, the QUASAR methodology involves the following steps: (a) selection of the important uncertainty parameters for a phenomenon of interest, (b) definitions of the ranges and distributions of uncertainty parameters, (c) sampling and combination of the uncertainty parameters, (d) calculation of the code, and (e) statistical analysis of the results (based on a regression technique). Various approaches have been derived from QUASAR, depending on the various sampling and quantification methods. Recently, significant efforts have been invested in reviewing and optimizing the methodologies for the quantification of the uncertainty and sensitivity of the currently available SA codes, e.g., through international joint projects such as "Management and Uncertainties of Severe Accidents" [19].

In 2019, International Atomic Energy Agency launched the Cooperative Research Project (CRP) I31033, entitled "Advancing the State-of-Practice in Uncertainty and Sensitivity Methodologies for Severe Accident Analysis in Water-Cooled Reactors" [20]. The goals were to advance the understanding and characterization of various sources of uncertainty, and to investigate their effects on the key figures-of-merit for SA code predictions for water-cooled reactors. Moreover, the Korea Atomic Energy Research Institute and Hanyang University participated in the project, and shared the results and insights based on the SA analysis of 1000 MWe optimized power reactor (OPR)1000 [21]. Notably, in the first year, the SA analysis of one unmitigated and two mitigated scenarios under a short-term station blackout (STSBO) accident were performed for the OPR1000 [22] using the latest versions of two SA analysis codes, i.e., MELCOR 2.2 [23] and MAAP 5.05 [24].

As implemented through the aforementioned CRP [20,22], the primary objectives of this study were to present the best-practice uncertainty and sensitivity analysis results on the evolution of the SAs and FP source terms, as well as to determine the effects of the SA mitigation measures expected during an STSBO of the OPR1000 plant using MELCOR 2.2. For this purpose, the present study considered three reference scenarios related to STSBO accidents: one base scenario and two mitigation scenarios. The uncertain model input parameters (i.e., the 26 addressed in the MELCOR code) were considered, covering both the in-vessel and ex-vessel accident phases of the SAs. The state-of-knowledge (epistemic) uncertainty in the model parameters was characterized as a probability distribution, thereby indicating that some values in the uncertainty ranges were more likely to be appropriate parameter values than others. Monte Carlo samples (100 per case scenario) were utilized to quantify the uncertainties addressed in the results of interest (i.e., the FOMs). The relative sensitivity/importance values of the individual model parameters for each relevant FOM were evaluated based on relevant sensitivity/importance measures [32].

2. Analysis methods

2.1. Reference code

Developed by the Sandia National Laboratories, MELCOR [23] is a fast-running integral code applicable for plant risk assessments during SAs in light water reactors. One of the key characteristics of the code is the use of both parametric and mechanistic models to simulate complex SA phenomena in a unified framework, as implemented with numerous subpackages. The code simulates the SA progress based on physicochemical phenomena such as the thermal-hydraulic behavior of the plant, core heat-up, oxidation and melting, relocation of the in-vessel molten corium, pressure boundary failure(s), and FP behavior including transport, sedimentation, and release. In this study, the simulation of the SAs was performed using MELCOR 2.2.11932.

2.2. Reference plant

The reference plant OPR1000, a representative operating PWR in Korea, was selected for the MELCOR simulation. The OPR1000 is equipped with two reactor coolant system (RCS) loops, two steam generators (SGs), two reactor coolant pumps per loop, and one pressurizer. The nominal thermal power is 2,815 MWt (1,000 MWe), with a low U-235 enrichment fuel below 4%. The containment building comprises an inner steel containment wall with an outer concrete building enveloping the nuclear steam supply system (NSSS), as a final barrier against FP release. The design leak rate of the containment is 0.2% of the total daily gas volume. The major design parameters used for the OPR1000 were identified in a previous study [22], and are summarized in Table 1. A schematic of the OPR1000 is shown in Fig. 1.

2.3. MELCOR modeling

(1) Reactor coolant system (RCS) nodalization

The MELCOR hydrodynamic nodalization of the NSSS for the

Table 1
Major design parameters of the reference plant [22].

Category	Parameter	Value
Power	Reactor Power	2,815 MWt (1,000 MWe)
Reactor core	Equivalent core diameter	3.5 m
	Active core height	3.8 m
	Number of fuel assemblies	177
	Fuel type	UO_2
	U-235 fuel enrichment	1.28−3.34 wt%
	Cladding material	Zircaloy-4/Zirlo
	Fuel rod array	16 × 16
	Number of control rods per fuel assembly	4 or 12
	Absorber material	B_4C/Inconel
Primary system	Number of coolant loops	2 (two reactor coolant pumps (RCPs) per loop)
	Core flow rate	15.3 t/s
	Coolant operating pressure	15.5 MPa
	Coolant inlet temperature	295.8 °C
	Coolant outlet temperature	327.3 °C
	Operating temperature (avg.)	311.6 °C
	Soluble poison in coolant	Boric acid
Secondary system	Steam pressure	7.4 MPa
	Steam temperature	285 °C
Containment	Design leak rate	0.2 % vol/day
	Design pressure	0.494 MPa
	Operating pressure	0.1 MPa
	Free volume	7.72×10^4 m^3
	Rector cavity (composition)	Basaltic concrete
	Rector cavity (thickness)	4.57 m (axial) / 2.6 m (radial)
Pipe/component/structure material	HL pipe	Carbon steel (SA 508)
	Pressurizer surge line	Stainless steel (SS 316)
	Steam generator U-tube	Inconel 600
	Reactor pressure vessel lower head	Carbon steel

HL, Hot leg; RCP, reactor coolant pump.

OPR1000 is shown in Fig. 2. A total of 54 control volumes (CVs) were constructed to model the RCS, including the safety injection system. For the RCS subsystem, a RPV was divided into five parts: the lower plenum (CV150), reactor core (CV170), downcomer (CV130), core bypass (CV180), and upper plenum (CV260). In addition, the hot leg (HL), SG tube, and SG inlet plenum were divided to simulate the natural circulation of hot gas from the core. The HL was divided into the upper hot part (CV310/CV320) and lower cold part (CV311/CV321). Each part had an opposite flow direction during natural circulation. Although the volumes of the upper and lower parts did not communicate with each other, the momentum exchange was considered via using the counter current flow limit model implemented in MELCOR [23]. The SG tube was also divided into hot upflow (CV340/CV347) and cold downflow (CV341/CV348) regions. The SG inlet plenum was divided into three parts: hot, cold, and mixing regions. The natural circulation modeling approach and split ratio were defined based on previous studies by Liao and Vierow [26] and Jung et al. [27], respectively. Table 2 summarizes the split ratio of the compartments for the natural circulation modeling.

The pressurizer (CV500) was modeled to be connected to the HL through a surge line (CV510). Two pilot-operated relief valves (PORVs) of the safety depressurization system (SDS) for depressurizing the RCS and a passive pressurizer safety relief valve (PSRV) were modeled on top of the pressurizer. All the safety valves of the pressurizer were connected to the reactor drain tank (RDT). The opening and closing set-points of the PSRV were 17.24 and 14.1 MPa of RCS pressure, respectively. Similar to the pressurizer, two pilot-operated safety valves were used the atmospheric dump valve and condenser dump valve, respectively, and passive safety valves for the main steam safety valve (MSSV) were modeled on top of each SG (CV600/700). Each SG was connected to a turbine (CV740) via the main steam isolation valve. The opening and closing set-points of the MSSV were 8.91 and 8.6 MPa of the SG pressure, respectively.

(2) Core nodalization

The nodalization of the reactor core is shown in Fig. 3. The reactor core was divided into 16 axial rings and 8 radial rings. Five axial nodes from the bottom were allocated to the lower plenum (CV150) and nine axial nodes above the lower plenum were assigned to the active fuel region, which included the UO_2 fuel and cladding. The last node at the top of the core was defined as the assembly upper region, where the core exit temperature was detected using a K-type thermocouple. The active fuel and assembly upper regions were allocated to the core volume (CV170).

(3) Containment nodalization

Fig. 4 shows the hydrodynamic nodalization of the reactor/containment building. A total of 77,500 m^3 of the free volume for the containment building was divided into 19 compartments, considering the locations of the plant features. The upper part of the containment (above a height of 11.89 m) comprised four CVs as a dome. Between -5.53 m and 11.89 m height, the annulus of the containment building was modeled, including the recirculation sump (CV831-833/CV836-838), SG compartment (CV821/CV822), containment door (CV812), annulus surrounding the RPV (CV823), pressurizer room (CV826), refueling pool (CV824), RDT room (CV850), and heat exchanger room (CV825). For the basement of the containment building, the reactor cavity (CV810) was modelled by considering the MCCI. To control the hydrogen concentration, 21 units of passive autocatalytic recombiners were modeled in the lower part of the dome (CV841/846) and in the upper part of the containment annulus (CV833/CV838). Although the hydrogen igniters were modeled in the SG compartment (CV821/822), RDT room (CV850), and cavity door (CV812), they were assumed to be unavailable in this study.

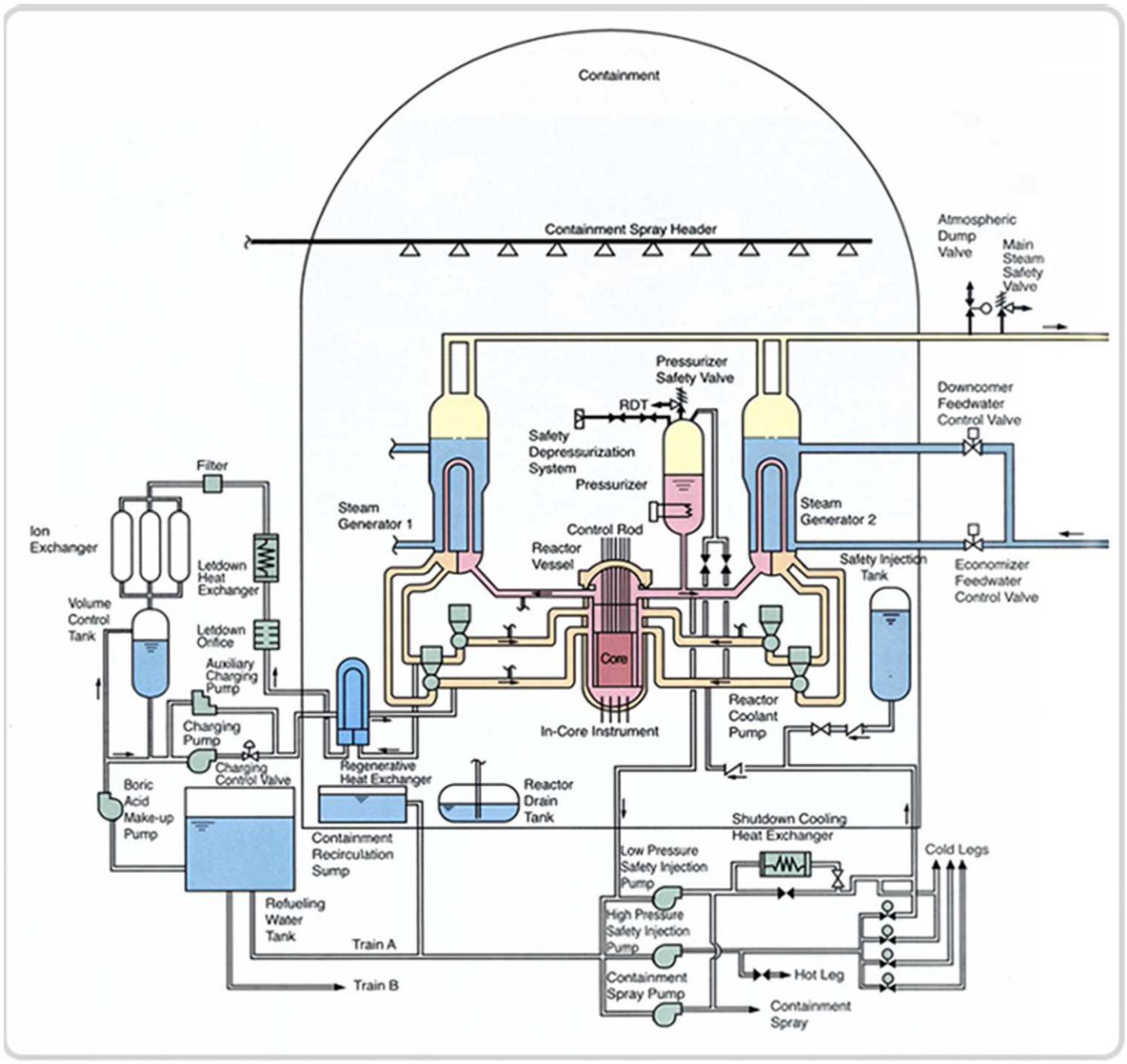

Fig. 1. Schematic of the 1000 MWe optimized power reactor (OPR1000) [25].

2.4. Reference scenarios

In this study, an uncertainty and sensitivity analysis was conducted for three reference scenarios: one unmitigated SA and two SAs mitigated by the relevant SA guidelines (SAGs). The initiating event of the unmitigated SA was defined as a "short-term SBO" (STSBO) [14]. The accident was initiated by the loss of onsite and offsite power, which led to the loss of secondary heat removal and other safety features, such as the high-pressure injection system and low-pressure injection system. In addition, the turbine-driven auxiliary feed water pumps were assumed to be unavailable during the accident, i.e., when the core degradation occurred rapidly. Because all the safety injection systems driven by alternating current power were unavailable, the mitigating actions to compensate for the RCS coolant inventory in the other two mitigated SA scenarios were assumed to be performed by an external mobile pump. The mitigating actions for the first case (Case 1) were defined as an external water injection into the RCS through an external mobile pump (SAG-3), and the removal of steam through the manual opening of the PORVs in the SDS (SAG-2). The second mitigation action (Case 2) was defined as the external water injection (EWI) into the SGs through the external pump and the removal of steam through the manual opening of the atmospheric dump valve (SAG-1). The other detailed assumptions for the mitigating actions are summarized in Table 3.

2.5. Figures-of-merit (FOMs) of interest

The present uncertainty analysis considered the following seven FOMs.

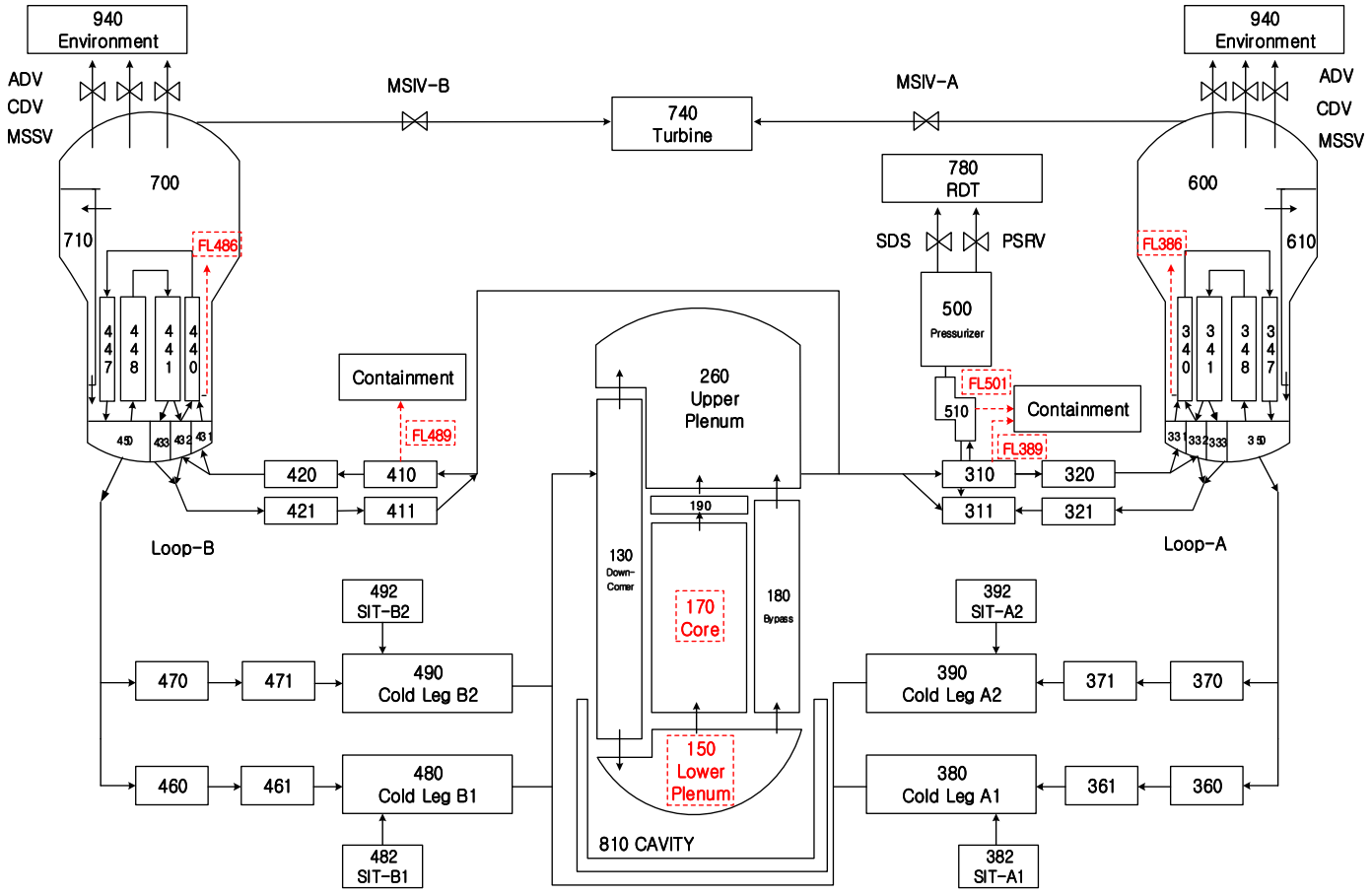

Fig. 2. MELCOR nodalization of nuclear steam supply system (NSSS) for OPR1000.

Table 2
Split ratios of compartment for natural circulation modeling.

Compartment	Split ratio	Description
Hot leg (HL)	50:50 (Upper:Lower)	- Volume of HL - Flow area from relief valve to HL
Steam generator (SG) inlet plenum	5:90:5 (Hot:Mixed:Cold)	- Volume of SG inlet plenum - Flow area from HL to SG inlet plenum
SG tube	35:65 (Hot:cold)	- Volume of SG tube - Flow area from SG inlet plenum to SG tube

SG, steam generator; HL, hot leg.

(1) Time to core (top of active fuel) uncovery (FOM 1)
(2) Time to RPV lower head (LH) failure (FOM 2) and reactor/containment building failure (FOM 3)
(3) Generation of flammable gases [hydrogen (FOM 4, FOM 5) and carbon monoxide (CO, FOM 6)] in the in-/ex-vessel accident phases
(4) Release fraction of the FP source terms into the environment (Cs) (FOM 7).

The foregoing FOMs are closely related to the risk metrics or risk-informed safety goals of nuclear power plants. More specifically, FOM 1 is commonly used to estimate the core damage frequency, and the remaining FOMs are used to evaluate the large early release frequency /large release frequency.

2.6. Uncertainty input parameters

The MELCOR code allows for modification of the parameters in the physical correlations, via the sensitivity coefficient or input parameters [23]. In this study, 26 uncertainty parameters were selected to analyze their effects on the uncertainty of the relevant FOMs: one for the decay heat of the FP, 18 for in-vessel phenomena, one for the heat transfer to the containment concrete wall, three for the ex-vessel debris bed cool ability and MCCI, one for the combustion of flammable gas, and two for FP release and transport. The ranges and probability distributions of the uncertainty parameters were defined based on previous work [9,14,17,28] or engineering judgements. Table 4 summarizes the probability distributions assigned to the uncertainty parameters.

2.7. Uncertainty and sensitivity analysis methods

The present uncertainty analysis focused mainly on clarifying and quantifying the uncertainty in the code output, owing to the uncertainties addressed in the code input parameters (i.e., the parameter-driven uncertainty). The results from the uncertainty

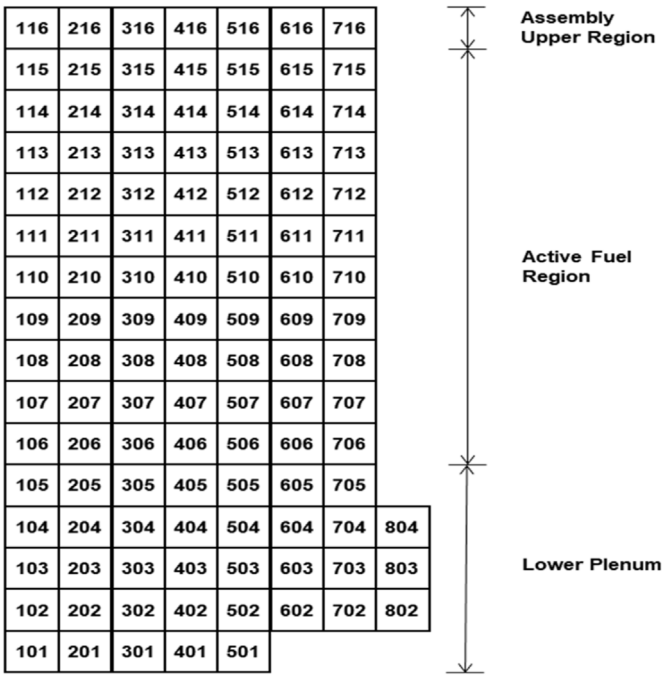

Fig. 3. Nodalization of reactor core.

analysis were expected to account for the combined influences of all identified input uncertainties on the results.

Fig. 5 shows a schematic of the uncertainty and sensitivity analysis process applied in this study. Under the Symbolic Nuclear Analysis Package (SNAP) environment [29], the sampling of the uncertainty parameters, generation of the input files, and calculations with the MELCOR code were performed by using the Design Analysis Kit for Optimization and Terascale Applications (DAKOTA), which is implemented as a SNAP plug-in [30]. It is well-known that Latin Hypercube Sampling (LHS) is an effective methodology for sampling. However, LHS is unusable when the arbitrary sample calculation fails, as it requires the stratification of the input space [14]. In other words, LHS technique is not recommended for the uncertainty and sensitivity analysis of the results obtained from MELCOR due to the elevated failure probability of the calculation. Thus, in this study, simple random sampling was used to generate the input files for each reference scenario. Subsequently, the uncertainties of the input parameters were propagated through the MELCOR code, that is, through probabilistic simulations. In this process, the input parameters considered in the uncertainty analysis were assumed to be independent of each other. This implies that the samples of each input parameter were not correlated each other to prevent the multicollinearity problem [31]. The underlying statistical values [such as the 5^{th} and 95^{th} percentiles, mean, median (50^{th} percentile), and standard deviation] were derived to help consider the uncertainties of each relevant FOM. Finally, the sensitivity/importance values of the uncertainty parameters on each relevant FOM were quantified using both the correlation-based and regression-based approaches adopted by Ahn et al. [32], as follows.

(1) Correlation-based importance measures: Pearson and Spearman rank correlation coefficients.
(2) Regression-based importance measures: partial correlation coefficient, partial rank correlation coefficient (PRCC), standardized regression coefficient, and standardized rank regression coefficient (SRRC).

While the forgoing correlation-based approaches assume a linear and/or monotonic relationship between inputs and outputs and the linear regression-based approaches have the advantage of being robust if they well represent a given model, they are unable to capture well complex nonlinear and/or non-monotonic relationships between inputs and the relevant outputs. However, these coefficients are easy intuitively understand the influence of model inputs on the relevant outputs, and thus they have been widely used in many engineering fields. Using such a suite of coefficients could also allow for better coverage of potential relations between inputs and outputs. The estimated correlation coefficient in between 1.0 and 0.7, 0.7 and 0.3, 0.3 and 0.1, and 0.1 and 0 in terms of its absolute value, represents very strong, strong, weak, and little or no relationship, respectively.

3. Analysis results

For the three reference scenarios, the code simulations were run for 72 h after the STSBO accident. Monte Carlo sample calculations of N = 200 per case scenario were adopted in the present study in

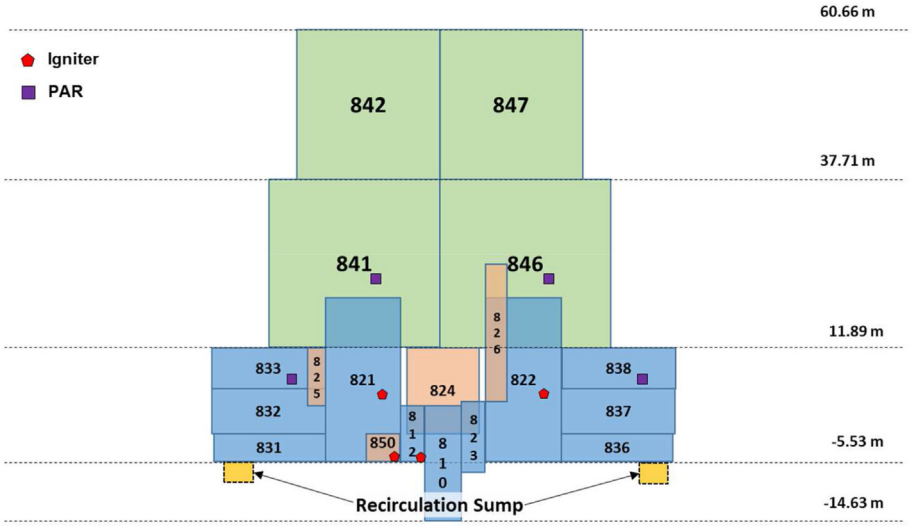

Fig. 4. Nodalization of containment building.

Table 3
Three reference scenarios selected for the present study.

Base (unmitigated) Case	Mitigation Case 1 (Severe accident guideline (SAG)-3: Reactor coolant system (RCS) water level control)	Mitigation Case 2 (SAG-1: SG water level control)
- Loss of onsite and offsite power and emergency diesel generator (EDG) (No AC power recovery) - Turbine-driven auxiliary feedwater and motor-driven auxiliary feedwater (motor-driven auxiliary feedwater) pumps are unavailable - Safety injection system (SIS) is unavailable except for four safety injection tanks (SITs) - The failure of the RCP seal is not considered - Passive autocatalytic recombiners are available to remove hydrogen in the containment - Hydrogen ignitors are assumed to be unavailable	Power supply from the mobile EDG at 4 h after the accident to run dedicated external mobile pumps - Open two pilot-operated relief valves (PORVs) of safety depressurization systems (SDSs) to depressurize the RCS (SAG-2) when core exit temperature (CET) reaches the severe accident management guidance (SAMG) entry condition (CET: 923.15 K) - Close the valves of SITs to prevent the inflow of nitrogen into the RCS at the RCS pressure of 1.196 MPa (12.1 kg/cm^2) - Inject the emergency feedwater into the RCS at 4 h after the accident using external mobile pump	- Close the two SDS valves to derive a natural circulation through the RCS loop just after SIT injection stops - Open two atmospheric dump valves (ADVs) of the SG-A at 4 h after the accident - Inject the emergency feedwater into the SG-A secondary side using dedicated mobile pump

SAG, severe accident guideline; RCS, reactor coolant system; EDG, emergency diesel generator; PORV, pilot-operated relief valve; SDS, safety depressurization system; CET, core exit temperature; SAMG, severe accident management guidance; SIS, safety injection system; SIT, safety injection tank; ADV, atmospheric dump valve.

consideration of the time-consuming code predictions (which could be on the order of several hours per sample calculation for plant applications), as well as to account for unexpected code crashes. Among the 200 Monte Carlo samples tested in the present study, more than 30% failed code runs. The failed code runs were random, did not share any specific tendencies, and were manually discarded. The underlying reasons could be owing to either combinations of physically unreasonable random values beyond the capability of the MELCOR code or a numerical problem, by which the relevant thermal-hydraulic behavior did not numerically converge. Accordingly, failed code runs were manually discarded from the analysis for the relevant FOMs. Among the normal calculations, 100 samples per case scenario were used for processing the MELCOR results. For reference, the sample size of 100 slightly exceeds the minimum sample size of 93 required for the 2nd order Wilks formula at the one-sided 95%/95% tolerance limit [33].

3.1. Uncertainty analysis results

The three reference values estimated based on the best-estimate point values and mean values derived from the corresponding uncertainty analyses are summarized in Tables 5 and 6. Before taking mitigation actions, the key event timings for the three reference cases and means of the uncertainty cases showed almost identical trends. After the core exit temperature reached the entry point of the SAM Guidance (SAMG), each mitigation action in the two mitigated cases led to a different accident progression trend. Some key events, such as the HL creep rupture, oxidation, cladding failure, and RPV failure, were observed depending on the underlying uncertainty input parameters under consideration, although these were not observed in the reference calculations for the mitigated cases (see Table 5). When the occurrence of key events in the uncertainty calculation occurred in less than 10 samples, the present study did not consider the means of the corresponding key events. Likewise, some mean values of the mitigated cases were also not considered, owing to the small amount of data (below 10 samples). Detailed descriptions of the results of interest are provided in the following section.

3.1.1. Base (unmitigated) case

Before continuing the discussion on the statistics of the unmitigated case, it is important to define each relevant FOM explored in this study as follows:

(1) FOM 1: Core uncovery time

During the accident scenario defined in this study, the RCS coolant was discharged through the PSRV under the loss of secondary heat removal and the high-pressure conditions of the RCS. When the submerged fuel was exposed owing to the decrease in the water level, the exposed part of the fuel was heated, but with insufficient heat removal. Therefore, in this study, the beginning of the core uncovery was defined as a FOM to analyze the initiation of core heat up. The definition of the core uncovery time was when the water level of the core (CV170) reached the top of active fuel after the initiation of the accident.

(2) FOM 2: RPV failure time

When the melted fuel relocated to the lower region of the RPV, the inner surface was heated by the molten corium. In this situation, the RPV could fail, owing to creep rupture or penetration failure. The MELCOR code modeled each failure mechanism using the Larson-Miller creep rupture model, and a temperature-based parametric model [23]. In this study, the default creep rupture model had a sensitivity coefficient of 1601_4 (total strain assumed to cause failure), and the “TPFAIL” failure temperature was used as the temperature criteria for the penetration failure. Accordingly, the sensitivity coefficient 1601_4 and TPFAIL were the uncertainty parameters to be analyzed in this study. There could be multiple failures for each core ring, but the first failure time was used as the RPV failure time.

(3) FOM 3: Containment failure time

After the failure of the RCS pressure boundary, the containment pressure could be increased by the steam released from the RCS. In addition, the non-condensable gas from the MCCI could also accelerate an increase in containment pressure, leading to a rupture of the containment. When the containment pressure reached 0.9632 MPa, the flow path with a 0.1 m^2 flow area was modeled to open to the environment as a containment failure. The containment failure time indicated the timing of the flow-path opening. In this study, the leakage rate was defined as 0.2 vol% per day for intact containment.

(4) FOM 4: In-vessel H_2 generation

The Zr cladding and steel components in the core could potentially be oxidized by hot steam. In this oxidation process, additional heat and H_2, i.e., combustible gases, could also be generated. In

Table 4
Model parameters and relevant probability density functions (PDFs) considered for the uncertainty analysis.

Parameter	Range	Best estimate values	Distribution (PDF)
SC3200_1 *Multiplier for American Nuclear Society decay heat curve*	0.9–1.1	1.0	Uniform
PORDP *Porosity of particulate debris*	0.1–0.5	0.4	Lognormal $\mu = -0.85$, $\sigma = 0.32$
DHYPD *Particulate debris equivalent diameter*	0.01–0.06 m (Lower Plenum (LP) region) 0.002–0.05 m (core region)	0.002 m (LP region) 0.01 m (core region)	Lognormal (LP region) $\mu = -3.68$, $\sigma = 0.5$ Lognormal (core region) $\mu = -4.34$, $\sigma = 0.58$
VFALL *Velocity of falling debris*	0.01–1.0 m/s	0.01 m/s	Uniform
HDBH2O *Heat transfer coefficient from in-vessel falling debris to pool*	200–2000 W/m^2/K	2000 W/m^2/K	Uniform
COR_CHT_n *Candling heat transfer coefficient for UO2, Zr, and ZrO2 (n = UO2) or Steel, Steel oxide and poison (n = SS)*	2000–22000 W/m^2/K (UO_2 + Zr + ZrO_2) 500–8000 W/m^2/K (Steel + Steel Oxide + Poison)	7500 W/m^2/K (UO_2 + Zr + ZrO_2) 2500 W/m^2/K (Steel + Steel Oxide + Poison)	Lognormal $\mu = 9.04$, $\sigma = 0.63$ (UO_2 + Zr + ZrO_2) Lognormal $\mu = 7.9$, $\sigma = 0.83$ (Steel + Steel Oxide + Poison)
FUOZR *Transport parameters for UO_2 in molten Zircaloy*	0.0–0.5	0.2	Triangular Mode = 0.2
FCELn *Radiative exchange factor for radiation for axially upward (n = A) or radially outward (n = R)*	0.02–0.18	0.1	Normal Mean = 0.1, Std = 0.0375
HDBPN *Heat transfer coefficient from debris to penetration*	100–1000 W/m^2/K	100 W/m^2/K	Uniform
TPFAIL *Failure temperature of the penetrations or lower head*	1273.15–1686.15 K	1273.15 K	Uniform
SC1020_n *Time constant for the relocation of solid material (n = 1) or liquid material (n = 2)*	100–1000 (Solid) 10–100 (Liquid)	300 (Solid) 10 (Liquid)	Uniform
SC1131_2 *Maximum ZrO_2 temperature permitted to hold up molten Zr in cladding*	2100–2540 K	2400 K	Scaled Beta $\alpha = 3.83$, $\beta = 3.00$
SC1132_1 *Temperature to which oxidized fuel rods can stand in the absence of unoxidized Zr in the cladding*	-	2500 K	Normal Mean = 2479, Std = 83
SC1141_2 *Maxium melt flow rate per unit width after breakthrogh*	0.1–2.0 kg/m-s	1.0 kg/m-s	Logtriangular Mode = 0.2
SC1601_4 *Total strain assumed to cause failure*	0.16–0.20	0.18	Uniform
HTRBOT *Multiplier on the debris-to-surface heat transfer at the bottom surface of the debris*	0.9–2.0	1.0	Triangular Mode = 1
HTRSIDE *Multiplier on the debris-to-surface heat transfer at the side surface of the debris*	0.9–2.0	1.0	Triangular Mode = 1
COND.CRUST *Multiplier on the thermal conductivity of the crust*	1.0–5.0	1.0	Triangular Mode = 1
XH2IGN *H_2 mole fraction limit for ignition without igniter*	0.03–0.09	0.1	Discrete 0.04 = 0.33, 0.06 = 0.33, 0.09 = 0.33
CHI *Aerosol dynamic shape factor*	1.0–5.0	1.0	Scaled Beta $\alpha = 1.0$, $\beta = 5.0$
CHEMFORM *The fraction of cesium that transformed to Cs_2MoO_4*	0.0–1.0	0.8	Beta $\alpha = 9$, $\beta = 3$
XHTFCL *Calculated atmosphere heat transfer scaling factor*	1.0–2.0	1.4	Triangular Mode = 1.4

general, because the additional heat from oxidation can accelerate the core degradation, the mass of H_2 generated by oxidation is an important parameter for SAs. In this study, the in-vessel H_2 generation included the mass of the H_2 as generated by the oxidation of Zr and steel before RPV failure. The mass of H_2 generated from the oxidation of molten corium in the cavity after RPV failure did not include the in-vessel H_2 generation, but did include the ex-vessel H_2 generation.

(5) FOM 5: Ex-vessel H_2 generation and FOM 6: Ex-vessel CO generation.

After RPV failure, the molten corium relocated to the cavity could decompose the concrete into various non-condensable gases via MCCIs. Among the gases from the MCCIs, combustible gases such as H_2 and CO can affect containment integrity by combustion. In this study, the masses of H_2 and CO as generated by the MCCI were defined as the ex-vessel H_2 and CO generation.

(6) FOM 7: Cs release fraction to the environment

The radiological consequences of a SA are determined by the mass of the FPs released. Among FPs, Cs is a representative element

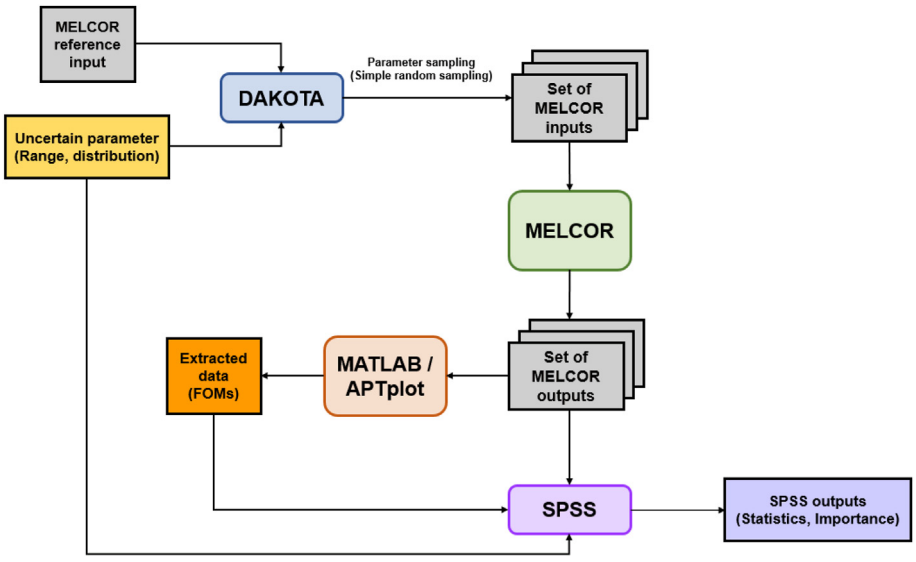

Fig. 5. Schematic of uncertainty and sensitivity analysis process.

Table 5
Key event timings (including figures-of-merit (FOMs)) (h).

Key events	Base Case (unmitigated)		Mitigated Case 1		Mitigated Case 2	
	Reference (best-estimate)	Uncertainty (mean)	Reference (best-estimate)	Uncertainty (mean)	Reference (best-estimate)	Uncertainty (mean)
Reactor, main feedwater (MFW), RCP trip	0					
Main steam safety valve (MSSV) first open	0.01					
All SGs dryout	1.02	1.03	1.02	1.04	1.02	1.02
Pressurizer safety release valve (PSRV) first open	1.39	1.40	1.39	1.41	1.39	1.38
Core uncovery (Reactor pressure vessel (RPV) water level < 6.127 m) **(FOM 1)**	2.09	2.11	2.09	2.13	2.09	2.08
SAMG entrance (CET > 923.15 K)	2.42	2.44	2.42	2.46	2.42	2.40
Opening of two SDS valves (Cases 1 and 2)	N/A	2.42	2.46	2.42	2.40	
Oxidation start	2.45	2.47	2.49	2.99	-	2.40[c]
Cladding failure (Fission product (FP) gap release)	2.49	2.52	3.56	3.53	–	3.77[d]
HL creep rupture	3.22	3.27	-	4.11[a]	-	-
SIT injection start	3.22	3.27	2.48	2.52	2.48	2.46
Opening of 2 ADVs (Case 1 only)	N/A				4.00	4.00
SIT injection stop	3.32	3.35	2.54	2.65	7.77	7.06
External water injection (EWI) (Case 1: RCS / Case 2: SG)	N/A		4.00	4.00	4.03	4.03
Failure of the core support plate	6.07	6.31	–	–	–	–
Corium relocation onto the RPV lower plenum	6.65	6.82	–	–	–	–
RPV failure **(FOM 2)**	6.77	7.30	–	– [b]	–	– [e]
Containment failure (Pressure > 0.9632 MPa) **(FOM 3)**	47.94	49.54	44.40	46.44	–	–

MFW, Main feedwater; MSSV, Main steam safety valve; PSRV, Pressurizer safety release valve; RPV, Reactor pressure vessel; FP, fission product; EWI, external water injection.
[a] 64 samples were observed with a mean value of 4.11 h.
[b] One sample was observed at 6.86 h.
[c] 54 samples were observed.
[d] 17 samples were observed.
[e] Four samples were observed with a mean value of 5.55 h.

Table 6
Generation of flammable gases and Cesium (Cs) release fraction (FOMs).

Key events	Base Case (unmitigated)		Mitigated Case 1		Mitigated Case 2	
	Reference (best-estimate)	Uncertainty (mean)	Reference (best-estimate)	Uncertainty (mean)	Reference (best-estimate)	Uncertainty (mean)
In-vessel H_2 generation (kg) **(FOM 4)**	573	445	226	191	–	(negligible)
Ex-vessel H_2 generation (kg) **(FOM 5)**	658	961	–	–	–	(negligible)
Ex-vessel CO generation (kg) **(FOM 6)**	972	1301	–	–	–	(negligible)
Cs release into the environment **(FOM 7)**	5.71E-2	5.83E-2	3.60E-3	3.92E-3	–	8.66E-4[a]

[a] Relevant Cs release was followed by the design leak rate of containment (0.2% vol/day) (observed in 16 samples, with four samples greater than 0.01), but not through the containment rupture.

representing a large proportion of the radiological consequences (especially the effective dose), owing to its long half-life and chemical characteristics. Therefore, the fraction of Cs released to the environment was defined as an FOM. It was defined according to the ratio of the initial inventory, and included the masses released through both leakage and rupture.

The results from the uncertainty analysis for the unmitigated STSBO are summarized in Table 7. The mean value of core uncovery (FOM 1) is close to the reference value of 2.09 h, and the mean values of the other FOMs regarding the key events (FOMs 2 and 3) are 0.5 and 1.6 h longer than the reference values, respectively. In the case of flammable gas generation, the mean value of in-vessel generation is 128 kg smaller than the reference value (FOM 4), but those of the ex-vessel generation are 303 and 329 kg larger than the reference values of FOMs 5 and FOM 6, respectively. The mean value of the Cs release fraction (FOM7) is slightly larger than the reference value, with a difference of 1.2E-3. The corresponding percentiles of each reference value for the FOMs (FOMs 1 to 7) area the lower 47th, 20th, 45th, upper 97th, lower 4th, 10th, and 45th percentiles on each cumulative distribution function (CDF), respectively. Fig. 6 shows the relevant CDFs for the FOMs.

3.1.2. Mitigated cases

As mentioned in Section 3.1, some key events not occurring in the reference calculations were observed in the mitigated Case 1. Although the mitigation actions (opening the SDS valves and EWI into the RCS) were performed in mitigated Case 1, a HL creep rupture was predicted in 64 samples, depending on the uncertainty parameters. The main reason for the HL creep rupture in mitigated Case 1 was attributed to both the thermal and pressure stresses on the RCS boundary, corresponding to 2–4 MPa of pipe stress and 1,500–1,600 K temperature peaks. Although the pressure stress of 2–4 MPa was relatively low, the creep rupture time as calculated by the Larson–Miller (LM) parameters steeply decreased to below hundreds or tens of seconds above 1,500 K. Therefore, HL the creep rupture in this low pipe stress could be initiated by the temperature peak. However, it is clear that the occurrence of the HL creep rupture was compensated for by the mitigation actions. Only one sample showed an RPV failure (FOM 2) regardless of the HL creep rupture in mitigated Case 1. In contrast, containment failures (FOM 3) was observed in all the uncertainty calculations for mitigated Case 1. The steam released from the RCS through the SDS or HL creep rupture overpressurized the containment to 0.9632 MPa, i.e., the criterion for containment rupture.

In mitigated Case 2, core degradation even to RPV failure was observed, even though core degradations, including cladding oxidation and failure, were not observed in the reference calculations. However, only 17 samples of this nature were observed and, among them, four samples were owing to cladding and RPV failures, respectively; this was despite observing 54 samples with oxidation. Notably, the generation of flammable gas in most of the uncertainty calculations of the mitigated Case 2 was negligible to below 1 kg, except for the samples with RPV failures. The main reason for cladding failures in certain samples could be the uncertainty of the decay heat and the efficiency of the SIT water. No HL creep rupture was observed in any of the calculations for mitigated Case 2. In contrast to mitigated Case 1, the containment pressure was maintained below the rupture criterion, owing to the secondary heat removal by the actions in mitigated Case 2.

The timing of the core uncovery (FOM 1) was the same for all three reference calculations. In addition, few (or no) samples were observed for the RPV failure (FOM 2) and ex-vessel flammable gases (FOMs 5 and 6) in the uncertainty calculations for the mitigated cases. In mitigated Case 2, insufficient numbers of samples were observed for both containment failure (FOM 3) and in-vessel flammable gases. Therefore, only the meaningful uncertainty analysis results for the mitigated cases are summarized in Table 8. The mean value of the containment failure (FOM 3) in mitigated Case 1 is approximately 2 h longer than the reference value. The mean value of the in-vessel hydrogen (FOM 4) is 35 kg, i.e., smaller than that of the reference calculation of 236 kg. The mean value of the environmental Cs release fraction (FOM 7) in mitigated Case 1 is slightly higher than the reference value. Nevertheless, the order of the released fraction is much smaller than the lower 5th percentile value of the unmitigated case. In the mitigated Case 2, only 16 samples show environmental Cs releases (FOM 7), with a mean value of 8.66E-4. Notably, there was no release in the reference calculation of the mitigated Case 2, and the release in the aforementioned 16 samples was caused by the design leakage of containment, not by the rupture. The corresponding percentile values of the reference calculations were the lower 45th percentile, upper 86th percentile, and lower 21st percentile for FOMs 3, 4, and 7 in mitigated Case 1, respectively. The relevant CDFs of the FOMs for the mitigated cases are shown in Fig. 7.

3.2. Sensitivity/importance analysis results

The four sensitivity/importance measures described in Section 2.6, that is, the Pearson and Spearman correlation coefficients and PRCC and SRRC, were evaluated to address the relative importance of the uncertain input parameters to each FOM. In the case of such regression-based measures (PRCC/SRRC), the importance measures are only meaningful with a coefficient of determination R^2 greater than 0.5, where the regression model explains above 50% of the output variance [32]. Figs. 8 and 9 summarize the underlying sensitivity/importance analysis results, including the relevant regression-based measures with R^2 values greater than 0.5. The major contributors among the uncertainty input parameters (those having stronger correlations with each relevant FOM than the others) are also provided in Table 9. For reference, the final contributors of these uncertainty inputs to each relevant FOM were determined by equally weighting the relevant correlation coefficients (i.e., a weighted average). The following sections summarize the potential influences of the relevant inputs on the FOMs of interest.

3.2.1. Core uncovery time (FOM 1, all three reference cases)

The core uncovery time (FOM 1) exhibits the same trend in both

Table 7
Uncertainty analysis results: unmitigated case.

FOM	5th percentile	Median	95th percentile	Standard deviation (SD)	Mean
FOM 1 [h (s)]	1.86 (6696)	2.10 (7560)	2.35 (8460)	0.16 (576)	2.11 (7596)
FOM 2 [h (s)]	6.53 (23508)	7.29 (26244)	8.10 (29160)	0.50 (1800)	7.30 (26280)
FOM 3 [h (s)]	42.17 (151812)	49.05 (176580)	57.35 (206460)	4.81 (17316)	49.54 (178344)
FOM 4 [kg]	374	440	533	53	445
FOM 5 [kg]	678	1014	1121	161	961
FOM 6 [kg]	874	1383	1547	240	1301
FOM 7 [-]	2.17E-2	6.13E-2	9.02E-2	2.21E-2	5.83E-2

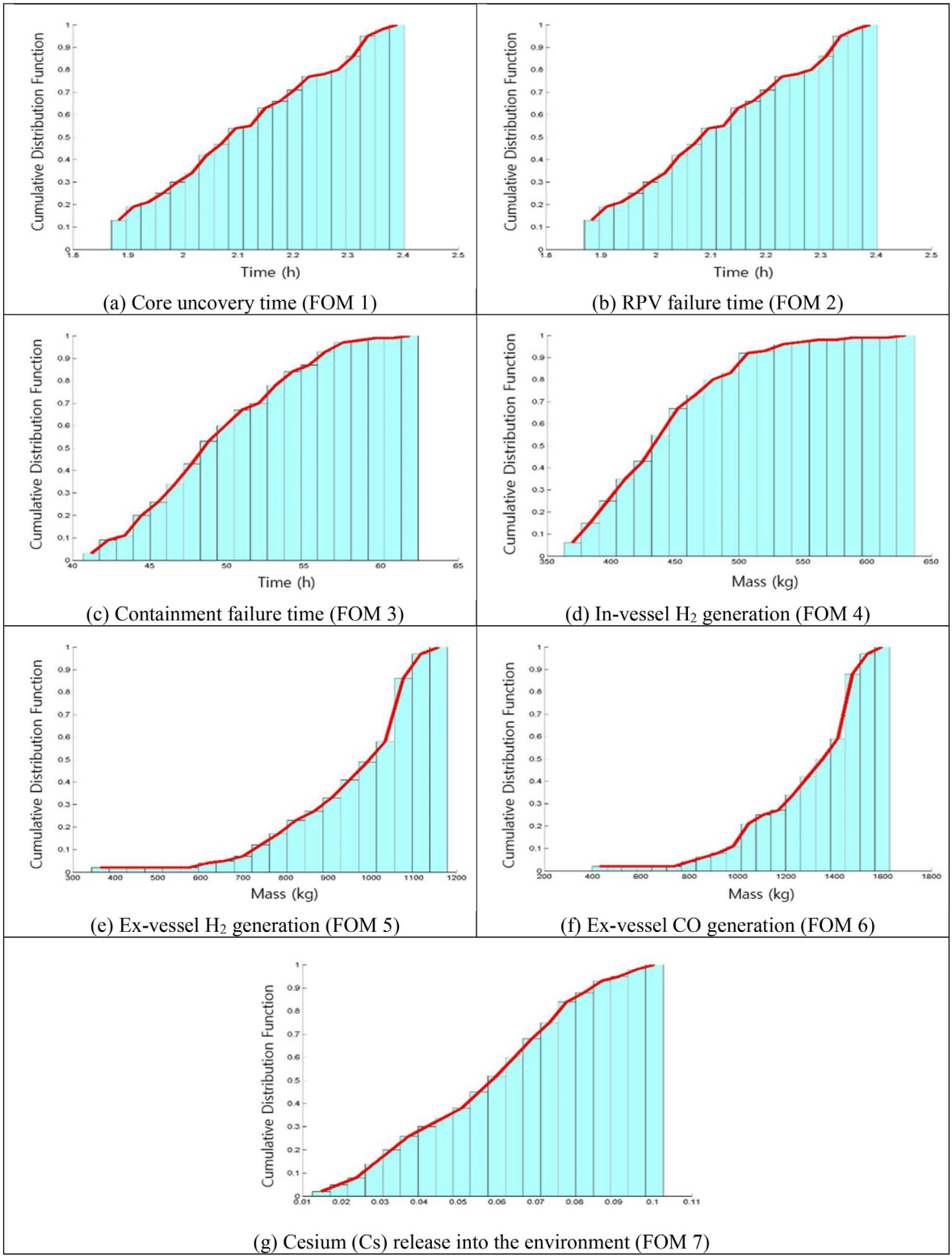

Fig. 6. Uncertainty analysis results: relevant cumulative distribution functions (CDFs) for the unmitigated case.

the unmitigated and mitigated cases. Because only the thermal-hydraulic phenomena affect the core heating and dry-out before the core degradation, SC3200_1 (proportional constant for decay heat calculation) is observed as the highest value of importance. A very strong negative correlation is observed (with less than -0.98) for all relevant coefficients, as shown in Fig. 8(a). The larger SC3200_1 simulates a larger decay heat, and therefore, the earlier core uncovery and damage appear, owing to the faster boiling of the coolant. The FCELR and FCELA, which are the parameters used to calculate the radiative heat transfer between fuel cells, also affect

Table 8
Uncertainty analysis results: mitigated Cases 1 and 2.

FOM	Cases	5th percentile	Median	95th percentile	SD	Mean
Containment failure time (FOM 3), h (s)	Mitigated Case 1	37.91 (136476)	47.66 (171576)	55.83 (200988)	5.93 (21348)	46.44 (167184)
In-vessel H_2 generation (FOM 4), kg	Mitigated Case 1	118	195	261	42	191
Cs release fraction to the environment (FOM 7)	Mitigated Case 1	1.80E-4	8.59E-4	1.66E-2	9.45E-3	3.92E-3
	Mitigated Case 2	–	–	1.01E-6	4.56E-3	8.66E-4

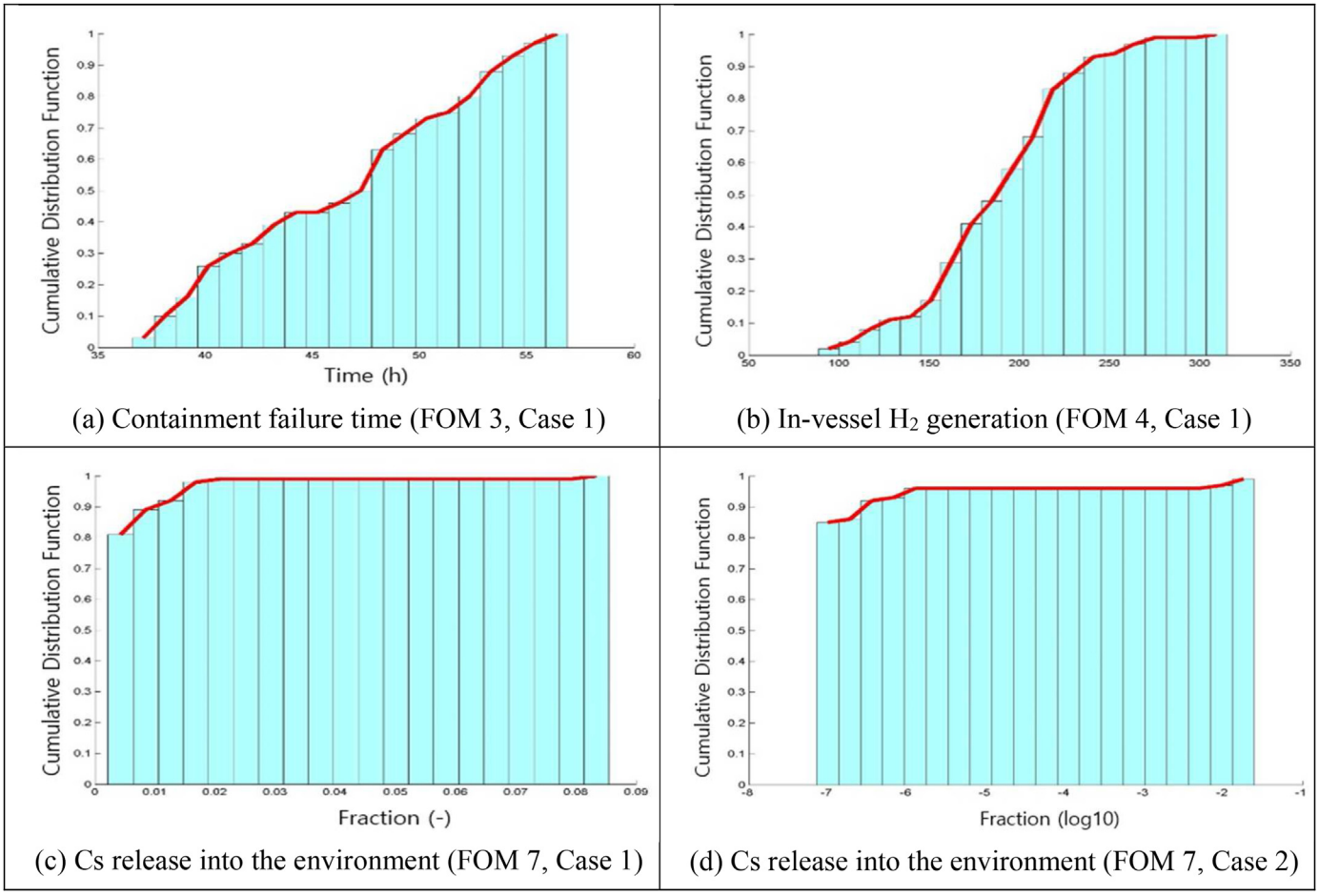

Fig. 7. Uncertainty analysis results, CDF, mitigated Cases 1 & 2.

FOM 1 by dissipating the core heat in the radiative heat transfer. However, the magnitude of these measures is less than 0.1, leading to a minor effect on FOM 1.

3.2.2. Reactor pressure vessel (RPV) failure time (FOM 2, unmitigated case only)

A significant number of RPV failures (FOM 2) are observed only in the unmitigated case. As shown in Fig. 8(b), SC3200_1 is also the most important contributor to FOM 2, with a very strong negative correlation (less than -0.85 for all relevant coefficients). Because the higher SC3200_1 causes more decay heat, the LH heating increases the temperature to reach the criteria of RPV failure, causing an earlier RPV failure. Although the magnitudes of the relevant measures are relatively lower than those of SC3200_1, the heat transfer coefficient from the debris to the penetration structures (referred to as "HDPBN") and candling heat transfer coefficient of the steel components (COR_CHT_SS) affect FOM 2 as the second and third contributors, respectively. The larger HDPBN results in a greater heat transfer to the penetration structures, leading to an earlier RPV failure by penetration failure. In contrast, the larger COR_CHT_SS causes a delay in RPV failure. With the increased candling heat transfer of the molten steel, the temperature increase of the steel structure supporting the fuel is disturbed, and therefore, the beginning of the LH heating is delayed with the delayed relocation of the molten corium. TPFAIL, the temperature criterion for the LH failure, is the fourth contributor to FOM 2. As shown by the positive correlation, the time to reach the temperature for RPV failure increases with higher values of TPFAIL. The fifth contributor is SC1020_2, i.e., the time constant for controlling the radial relocation of the molten corium. The higher SC1020_2 delays the relocation of the molten corium to the lower head because it causes radial relocation of the corium, rather than axial relocation. For the other parameters, the influence on FOM 2 remains unclear, owing to the significantly small relevant measures.

3.2.3. Containment failure time (FOM 3, unmitigated case and mitigated Case 1)

The structural failure of the reactor/containment building (FOM

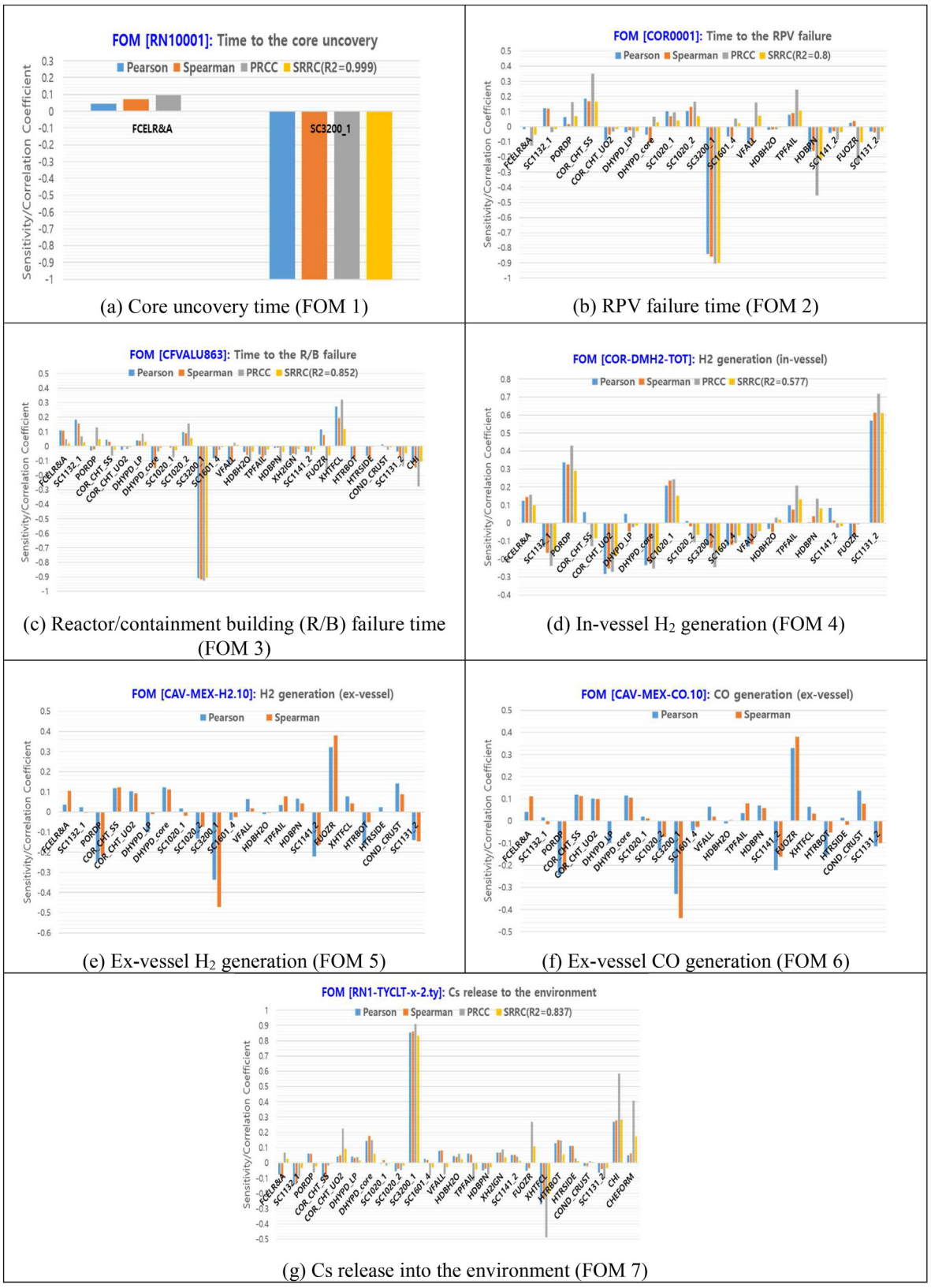

Fig. 8. Sensitivity analysis results for unmitigated case.

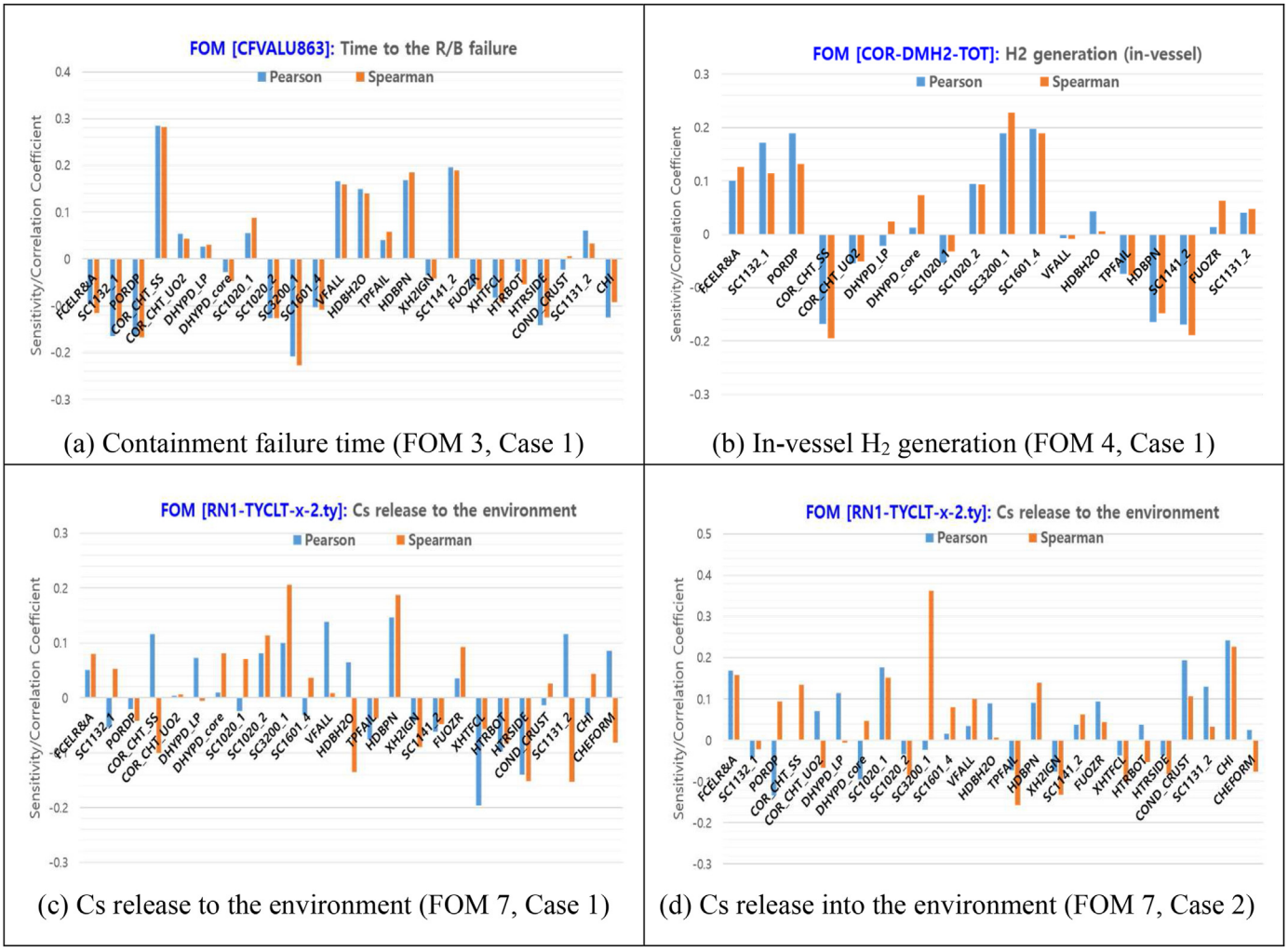

Fig. 9. Sensitivity analysis results for mitigated Cases 1 and 2.

Table 9
Key contributors to relevant FOMs (based on the equally weighted average of the relevant sensitivity/importance measures).

FOM	Case	Rank 1	Rank 2	Rank 3	Rank 4	Rank 5
FOM 1	All Cases	SC3200_1 (-1.00)	FCEL (+0.05)	-	-	-
FOM 2	Unmitigated Case only	SC3200_1 (-0.88)	HDBPN (-0.25)	COR_CHT_SS (+0.22)	TPFAIL (+0.13)	SC1020_2 (+0.12)
FOM 3	Unmitigated Case	SC3200_1 (-0.92)	XHTFCL (+0.23)	CHI (-0.16)	SC1132_1 (+0.11)	SC1020_2 (+0.10)
	Mitigated Case 1	COR_CHT_SS (+0.24)	VFALL (+0.22)	SC3200_1 (-0.21)	SC1141_2 (+0.20)	HDBPN (+0.19)
FOM 4	Unmitigated Case	SC1131_2 (+0.63)	PORDP (+0.35)	COR_CHT_UO2 (-0.25)	DHYPD_core (-0.22)	SC1020_1 (+0.21)
	Mitigated Case 1	SC3200_1 (+0.21)	SC1141_2 (-0.19)	SC1601_4 (+0.18)	HDBPN (-0.18)	COR_CHT_SS (-0.16)
	Mitigated Case 2	SC3200_1 (+0.60)	COND_CRUST (+0.22)	FCEL (+0.19)	COR_CHT_SS (+0.15)	HDBPN (+0.14)
FOM 5	Unmitigated Case only	SC3200_1 (-0.45)	FUOZR (+0.32)	PORDP (-0.21)	SC1141_2 (-0.14)	CHEFORM (-0.14)
FOM 6						
FOM 7	Unmitigated Case	SC3200_1 (+0.86)	CHI (+0.35)	XHTFCL (-0.30)	CHEFORM (+0.17)	DHYPD_core (+0.13)
	Mitigated Case 1	SC3200_1 (+0.19)	HDBPN (+0.19)	HTRSIDE (-0.15)	SC1020_2 (+0.14)	SC1131_2 (-0.11)
	Mitigated Case 2	SC3200_1 (+0.28)	CHI (+0.25)	SC1020_1 (+0.21)	TPFAIL (-0.19)	HDBPN (+0.17)

3) was observed in the unmitigated case and mitigated Case 1. The sensitivity analysis results for FOM 3 are shown in Figs. 8(c) and **9(a)**, respectively. The major contributors were different for the unmitigated case and mitigated Case 1, as shown in Table 9.

(1) Unmitigated case

SC3200_1 shows a very strong negative correlation (less than -0.9 for all relevant coefficients) as the first important contributor to FOM 3. The higher decay heat causes a greater amount of steam to be released from the core during the in-vessel phase, and a greater amount of non-condensable gas from the MCCI during the ex-vessel phase. As a result, a higher SC3200_1 accelerates the pressurization of the containment, leading to an earlier containment failure. For the second contributor to FOM 3, the higher the scale factor for heat transfer from the atmosphere to the concrete wall (referred to as the "XHTFCL"), the greater the removal of heat through the containment wall. Thus, this could contribute to the

delay in the containment failure. The third contributor to FOM 3 is the aerosol dynamic shape factor (denoted as "CHI"). CHI may affect the heat distribution owing to the sedimentation of the radioactive aerosol but its effect is unclear, owing to the relatively weak correlation (less than 0.3 for the magnitude of measures). A negative correlation is observed between the CHI and FOM 3. Likewise, the influences of the fourth contributor, i.e., the core component failure parameter (SC1132_1) and fifth contributor (SC1020_2) appear to be insignificant.

(2) Mitigated Case 1

Owing to the relevant actions in the mitigated Case 1, the major contributors to FOM 3 are slightly different in mitigated Case 1. COR_CHT_SS is observed as the first contributor, with a weak positive correlation (between 0.0 and 0.3 for all relevant measures). The second contributor to FOM 3 is the velocity of falling debris (denoted as "VFALL") which shows a weak positive correlation. The other contributors, ranked third to fifth, are SC3200_1, the core melt breakthrough candling parameter (SC1141_2), and HDBPN, as shown in Table 9. Notably, the regression model for FOM 3 in mitigated Case 1 shows a weak determination coefficient (less than 0.5 for R^2). Therefore, it may be insufficient to explain the influences of the selected uncertainty parameters on FOM 3 in mitigated Case 1.

3.2.4. In-vessel H_2 generation (FOM 4, unmitigated case and mitigated Case 1)

In-vessel H_2 generation (FOM 4) is also observed in both the unmitigated case and mitigated Case 1. The sensitivity analysis results for FOM 4 are shown in Figs. 8(d) and **9(e)**. The major contributors differ between the unmitigated case and mitigated Case 1, as shown in Table 9.

(1) Unmitigated case

The molten material holdup parameter (SC1131_2) is the most important contributor to FOM 4 in the unmitigated case. A strong positive correlation (greater than 0.55 for all relevant coefficients) is observed for SC1131_2. During the cladding oxidation process, molten Zr is held up in the oxidized cladding. Therefore, the fuel rod can maintain an intact geometry above the melting temperature of Zr. However, at higher temperatures, the oxidized Zr cladding can fail. In this case, the geometry of the fuel can be transformed due to the candling of the molten zircaloy, owing to the reduction in the reaction area. Because a higher SC1131_2 can delay the transformation of the intact fuel geometry, a greater amount of hydrogen can be generated without reducing the reaction area. The second and third contributors to FOM 4 are the porosity of the debris (PORDP) and candling heat transfer coefficients for the molten corium (COR_CHT_UO2), with weak (approximately 0.3 for the magnitude of all relevant coefficients) positive and negative correlations, respectively. The higher PORDP results in the larger surface area which causes the more oxidation with steam. In addition, the larger surface aera caused the cooling of the core debris, leading to a delay in the core geometry failure which can cause the reduction of surface area. Therefore, a greater amount of hydrogen can be generated with the larger surface area. In the case of COR_CHT_UO2, the higher COR_CHT_UO2 transfers more heat from the molten corium to the cladding. As a result, the blockage of the flow area by the molten corium occurs more easily, preventing the inflow of steam for oxidation. The particulate debris equivalent diameter in core region (DHYPD_core) is the fourth contributor, with a weak negative correlation (between -0.3 and 0 for all relevant coefficients). Higher values of DHYPD_core reduce the reaction's area-to-volume ratio, leading to a decrease in hydrogen generation from the debris. The time constant for controlling the radial relocation of the particulate debris (SC1020_1), SC1132_1, and SC3200_1 have some influence on FOM 4, but the magnitudes of their correlations are weaker than that of DHYPD_core.

(2) Mitigated Case 1

SC3200_1 is the most important parameter for FOM 4, with a weak positive correlation (between 0 and 0.3 for all relevant coefficients). Owing to the temporary core exposure in the mitigated Case 1, most of the in-vessel hydrogen generation in the mitigated Case 1 is observed between the initial core uncovery and the recovery of the core water level via the SIT injection. At this point, the higher SC3200_1 may cause a higher decay heat, leading to the acceleration of oxidation according to the high cladding temperature. Regarding the other contributors, SC1141_2, the LM creep rupture parameter for RPV steel (SC1601_4), HDBPN, and COR_CHT_SS are ranked second to fifth, respectively. These parameters may affect FOM 4 via a heat transfer process during oxidation. Nevertheless, their influences on FOM 4 are unclear, owing to their weak correlations and low R^2 values.

3.2.5. Ex-vessel H_2 and CO generation (FOMs 5 and 6, unmitigated case only)

Both H_2 and CO are generated from the ex-vessel MCCI, in a proportional relationship. Therefore, the condition of the in-vessel molten corium injected into the reactor cavity and heat transfer mechanism of molten corium in the reactor cavity can affect FOMs 5 and 6. From this point, SC3200_1 and the fractional local dissolution of UO_2 in the molten Zr (FUOZR) contribute to FOMs 5 and 6 by affecting the in-vessel molten corium conditions before ejection into the reactor cavity. They are ranked first and second, respectively. Similarly, the PORDP and SC1141_2 rank as the third and fourth contributors to both FOMs 5 and 6, respectively. These results show that the effect of the in-vessel molten corium condition could be stronger than that of the heat transfer mechanism of the ex-vessel molten corium, similar to the multiplier for the debris-to-surface heat transfer at the bottom surface of the debris (HTRBOT). To clarify the detailed reason for this result, further studies on the influences of the ex-vessel corium conditions and specified MCCI parameters for FOMs 5 and 6 will be conducted in the future.

3.2.6. Cs release to the environment (FOM 7, all three reference cases)

Cs releases into the environment (FOM 7) are observed in all three reference cases. The sensitivity analysis results for FOM 7 are shown in Fig. 8(g). The major contributors to each reference case are listed in Table 9. The order of the Cs release fraction is closely related to the containment failure as well as the release and transport of FPs in the in-/ex-vessel. For reference, the Cs release fraction in mitigated Case 2, where a containment failure is not observed, is significantly lower than that of the unmitigated case and mitigated Case 1 (refer to Tables 8 and 9).

(1) Unmitigated case

SC3200_1 is the most important contributor to FOM 7, with a very strong positive correlation (greater than 0.8 for all relevant coefficients). As described Section 3.2.3, for FOM 3, a higher SC3200_1 causes an earlier containment failure. In addition, the Cs release fraction continuously increases until FOM 7 (72 h), regardless of the containment failure time. From this point, the higher SC3200_1 value leading to the earlier containment failure causes a higher Cs release fraction with a longer time for the release

of the Cs. As the second and third contributors to FOM 7, CHI and XHTFCL show positive and negative correlations, respectively. Whereas a higher CHI can cause less sedimentation of the Cs, a lower XHTFCL can cause a greater delay in the containment failure. Consequently, the Cs released fraction can be increased by both a higher CHI and lower XHTFCL. The fraction of total available Cs in the fuel that becomes Cs_2MoO_4 (CHEFORM) and DHYPD_core show positive correlations, but their influences are relatively weak as the fourth and fifth contributors.

(2) Mitigated Case 1

In mitigated Case 1, although an RPV failure is observed for only one sample, containment failures are observed for all the tested samples. This implies that most of the Cs retained in the RCS and part of the initial inventory for Cs are released, depending on the progress of the core degradation during the in-vessel phase. As a result, most of the major contributors to FOM 7 in mitigated Case 1 are related to in-vessel phenomena. The first contributor is SC3200_1, similar to the unmitigated case, but the correlation is weaker than that of the unmitigated case. The other major contributors, ranked second to fifth, are HDBPN, HTRSIDE (an MCCI-related parameter), SC1020_2, and SC1131_2, respectively. However, the R^2 values for FOM 7 in mitigated Case 1 are lower than 0.3. Therefore, it is unclear whether the influences of these contributors are meaningful to FOM 7 in mitigated Case 1.

(3) Mitigated Case 2

A containment failure is not observed in mitigated Case 2. Therefore, the only path to releasing Cs is the design leakage of the containment in mitigated Case 2. Except for four samples with observed RPV failure, the release fraction of Cs is significantly lower, and with only minor core degradation. Similar to the base case, SC3200_1 and CHI are ranked as the first and second contributors to FOM 7 in the mitigated Case 2. These factors may affect the core degradation and sedimentation of Cs. Nevertheless, the influences on FOM 7 are unclear owing to the weak correlations and low R^2 values. Likewise, the influences of SC1020_1, TPFAIL, and HDBPN, ranked as the third to fifth contributors, are also unclear; their correlations are even weaker than those of SC3200_1 and CHI. Notably, only 16 samples were used to calculate the relevant coefficients, because the release of Cs in the other 84 samples was not observed.

4. Summary and conclusion

In this study, best-practice uncertainty and sensitivity analyses were performed to quantify the statistical uncertainties associated with FOMs of interest, and to determine the effects of dedicated SAM measures as expected based on MELCOR2.2 during an STSBO accident of OPR1000. For each case scenario, 26 code-specific uncertain model parameters, whose phenomenological domains covered both the in- and ex-vessel phases of SAs, were selected for the present study. The foregoing model parameters and relevant probability distributions were selected based on recommendations in the MELCOR user guide [23], previous studies including the US SOARCA study [9,11,14,28], engineering judgements, and parametric sensitivity studies wherever necessary. The uncertainties for the FOMs of interest were quantified using 100 Monte Carlo samples taken statistically from the probability distributions of the individual model parameters. The relative importance values of the individual model parameters statistically affecting each relevant FOM were evaluated based on four types of sensitivity/importance measures (Pearson and Spearman correlation coefficients and PRCC and SRRC).

The following points summarize the main results of the present analyses, along with relevant insights.

(1) Before introducing the SAMG, all three scenarios (unmitigated case and mitigated Cases 1 and 2) exhibited similar trends. Once the relevant mitigated actions were taken at the entry point of the SAMG, each mitigated case showed different trends. The mean values of the FOMs showed a greater or lesser difference compared to the corresponding reference cases, but also showed similar trends, depending on each scenario.
(2) In the unmitigated case, the reference values of the key events, especially the timings of core uncovery (FOM 1), RPV failure (FOM 2), and reactor/containment building failure (FOM 3), showed more conservative results compared with the mean of the uncertainty calculation. However, the generation of flammable gases (H_2 and CO, FOMs 4–6) in the reference calculation was greater than the mean of the uncertainty calculation. Nevertheless, the Cs release fraction (FOM 7) of the reference calculation was slightly lower than the mean of the uncertainty calculation.
(3) In mitigated Case 1, an HL creep rupture, which was not observed in the corresponding reference case, appeared in 64 samples. According to the foregoing results, the HL creep rupture could be initiated depending on the uncertainty of the relevant thermal hydraulic behaviors in the RCS, despite the mitigation action(s) taken for RCS depressurization. Similarly, minor core degradations, such as oxidation and cladding failures, which were not observed in the corresponding reference case, could occur depending on the uncertainties of in-vessel phenomena and decay heat (as. shown by the observation of oxidation and cladding failures in some uncertainty calculations). The foregoing results indicate that the physicals model for the thermal hydraulics, in-vessel phenomena, and decay heat must be deeply considered for the simulation of relevant mitigation actions.
(4) The results from the sensitivity analysis showed that the most important parameters for the in-/ex-vessel accident progressions and release of Cs into the environment were the decay heat. However, the importance of the decay heat was relatively low in the mitigated cases. In the case of the generation of flammable gases, SC1131_2 (the temperature of the oxidized cladding to hold up molten Zr) was the most important parameter in the unmitigated case. Unlike the unmitigated case, the decay heat showed a strong positive correlation in mitigated Case 2. Notably, the number of tested samples for calculating the relevant sensitivity coefficients could be insufficient for this specific FOM (e.g., FOM 7 of mitigated Case 2) despite a sufficient number of simulations. Therefore, careful consideration is required to determine the relative importance of the individual uncertainty parameters in these cases.
(5) Finally, four sensitivity/importance measures employed in this study capture just the linear or monotonic influences of the uncertainty inputs on relevant outputs of interest, but not potential nonlinear and/or non-monotonic influences between these inputs and outputs. For example, most of the unmitigated cases employed in this study were subject to the R^2 value less than 0.5, representing potential nonlinear and/or non-monotonic relationships between the inputs and relevant FOMs. In order to obtain more reliable insights into the relative importance of these inputs in the nonlinear and/or non-monotonic models, it seems be necessary to additionally explore the nonlinear regression approaches such as

quadratic regression or Multivariate Adaptive Regression Splines (MARS) [14].

Declaration of competing interest

The authors declare that they have no known competing financial interests or personal relationships that could have appeared to influence the work reported in this paper.

Acknowledgments

This work was supported by the International Atomic Energy Agency under the Coordinated Research Project award I31033 on Advancing the State-of-Practice in Uncertainty and Sensitivity Methodologies for Severe Accident Analysis in Water-Cooled Reactors, launched in 2019. This work was also supported by a National Research Foundation of Korea (NRF) grant funded by the Korean government (MSIT: Ministry of Science and ICT) (No. 2022M2D2A1A02061334). This work was also partly supported by the Nuclear Safety Research Program through the Korea Foundation of Nuclear Safety (KoFONS) using the financial resources granted by the Nuclear Safety and Security Commission (NSSC) of the Republic of Korea (No. 2003006-0120-CG100).

References

[1] K.B. Cady, V.K. Dhir, R.J. Witt, Peer review of models for lower vessel head heat transfer and larson-miller failure criterion proposed for implementation into MELCOR, ERI/NRC 94–202 (1994).
[2] M.P. Manahan, An improved zircaloy-steam reaction model for use with the MARCH 2 (meltdown accident response characteristics) code, in: Proceedings of the International Meeting on Light-Water Reactor Severe Accident Evaluation, Cambridge, MA, 28 Aug - 1 Sep, 1983.
[3] R.M. Ostmeyer, An Approach to Treating Radionuclide Decay Heating for Use in the MELCOR Code System, SNL, Albuquerque, NM, 1985. SAND84-1404, NUREG/CR-4169.
[4] M.T. Farmer, S. Lomperski, D. Kilsdonk, R.W. Aeschlimann, S. Basu, A summary of findings from the melt coolability and concrete interaction (MCCI) Program, in: Proceedings ICAPP '07, Nice, France, May 13-18, 2007.
[5] M.T. Farmer, B.W. Spencer, J.L. Binder, D.J. Hill, Status and future direction of the melt attack and coolability experiments (MACE) Program at argonne national laboratory, in: 9th International Conference on Nuclear Engineering (ICONE-9), Nice, France, April 8-12, 2001.
[6] D.R. Bradley, Modeling of heat transfer between core debris and concrete, in: ANS Proceedings of the 1988 National Heat Transfer Conference, Houston, TX, 1988, pp. 37–49.
[7] T.Y. Chu, M.M. Pilch, J.H. Bentz, J.S. Ludwigsen, W. Lu, L.L. Humperies, Lower Head Failurer Experiments and Analyses, U.S NRC, Washington, DC, 1999. NUREG/CR-5582, SAND98-2047.
[8] D.A. Powers, J.L. Sprung, C.D. Leigh, Isotopes, elements, and chemical classes, in: Fission Product Behavior during Severe LWR Accidents: Recommendations for the MELCOR Code System, SNL, Albuquerque, NM. (Unpublished), 1987.
[9] R.O. Gauntt, N.E. Bixler, K.C. Wagner, An Uncertainty Analysis of the Hydrogen Source Term for a Station Blackout Accident in Sequoyah Using MELCOR 1.8.5, SNL, Albuquerque, NM, 2014, pp. SAND2014–2210, https://doi.org/10.2172/1200657.
[10] M.R. Denman, D.M. Brooks, Fukushima Daiichi Unit 1 Uncertainty Analysis – Exploration of Core Melt Progression Uncertain Parameters – Volume II, SNL, Albuquerque, NM, 2015. SAND2015-6612.
[11] P. Mattie, et al., State-of-the-Art Reactor Consequence Analyses Project: Uncertainty Analysis of the Unmitigated Long-Term Station Blackout of the Peach Bottom Atomic Power Station, U.S NRC, Washington, DC, 2012. NUREG/CR-7155, SAND2012-10702P.
[12] S. Park, K. Il Ahn, Y. Song, Uncertainty analysis of the potential hazard of MCCI during severe accidents for the CANDU6 plant, Sci. Technol. Nucl. Install. 2015 (2015), https://doi.org/10.1155/2015/462941.
[13] R. Chang, J. Schaperow, T. Ghosh, Jonathan Barr, C. Tinkler, M. Stutzke, State-of-the-Art Reactor Consequence Analyses (SOARCA) Report, U.S NRC, Washington, DC, 2012. NUREG-1735.
[14] K. Ross, N. Bixler, S. Weber, C. Sallaberry, J. Jones, State-of-the-Art Reactor Consequence Analyses Project: Uncertainty Analysis of the Unmitigated Short-Term Station Blackout of the Surry Power Station, U.S NRC, Washington, DC, (Draft report), 2019.
[15] R. Gharari, H. Kazeminejad, N. Mataji Kojouri, A. Hedayat, M. Hassan Vand, Application of a severe accident code to the sensitivity and uncertainty analysis of hydrogen production in the WWER1000/V446, Ann. Nucl. Energy 152 (2021) 1–18, https://doi.org/10.1016/j.anucene.2020.108018.
[16] M. D'Onorio, A. Giampaolo, G. Caruso, F. Giannetti, Preliminary uncertainty quantification of the core degradation models in predicting the Fukushima Daiichi unit 3 severe accident, Nucl. Eng. Des. 382 (July) (2021) 1–22, https://doi.org/10.1016/j.nucengdes.2021.111383.
[17] S. Galushin, P. Kudinov, Analysis of the effect of MELCOR modelling parameters on in-vessel accident progression in Nordic BWR, Nucl. Eng. Des. 350 (2019) 243–258.
[18] M. Khatib-Rahbar, E. Cazzoli, M. Lee, H. Nourbakhsh, R. Davis, E. Schmidt, A probabilistic approach to quantifying uncertainties in the progression of severe accidents, Nucl. Sci. Eng. 102 (3) (Jul. 1989) 219–259, https://doi.org/10.13182/NSE89-A27476.
[19] L.E. Herranz, et al., The EC MUSA project on management and uncertainty of severe accidents: main pillars and status, Energies 14 (15) (2021) 1–11, https://doi.org/10.3390/en14154473.
[20] https://www.iaea.org/projects/crp/i31033.
[21] K.I. Ahn, Establishment of Best Practice for Uncertainty and Sensitivity Analyses in the Realm of Severe Accident Analysis and Development of Relevant TECDOC. 1st RCM on Advancing the State-Of-Practice in Uncertainty and Sensitivity Methodologies for Severe Acciden, IAEA Headquarters, Vienna, Austria, 2019.
[22] K.-I. Ahn, S.-Y. Park, W. Choi, S.J. Kim, Best-practice severe accident analysis for the OPR1000 short-term SBO sequence using MELCOR2. 2 and MAAP5, Ann. Nucl. Energy 160 (2021) 1–15.
[23] L.L. Humphries, B.A. Beeny, F. Gelbard, D.L. Louie, J. Phillips, MELCOR Computer Code Manuals, Vol. 1: Primer and Users' Guide. Version 2.2, SNL, Albuquerque, 2018. NM, SAND2018-13559.
[24] EPRI, Modular Accident Analysis Program (MAAP5.04). Fauske & Associates (FAI), vols. 1–4, Electric Power Research Institute, USA, 2016.
[25] KEPCO engineering & construction, "the schematics of OPR1000.". https://www.kepco-enc.com/eng/contents.do?key=1532. (Accessed 1 September 2021).
[26] Y. Liao, K. Vierow, Melcor analysis of steam generator tube creep rupture in station blackout severe accident, Nucl. Technol. 152 (3) (2005) 302–313, https://doi.org/10.13182/NT05-5.
[27] G.H. Jung, et al., Development of MELCOR 1.8.6 Input Decks for the OPR1000 Level 2 Phenomenological Uncertainty Analysis (I), KAERI, Daejoen, 2010. KAERI/TR-4113/2010.
[28] Y. Bang, G. Jung, B. Lee, K. Il Ahn, Estimation of temperature-induced reactor coolant system and steam generator tube creep rupture probability under high-pressure severe accident conditions, J. Nucl. Sci. Technol. 49 (8) (2012) 857–866, https://doi.org/10.1080/00223131.2012.703945.
[29] K. Jones, J. Rothe, W. Dunsford, Symbolic Nuclear Analysis Package (SNAP), U.S NRC, Washington, DC, 2009. NUREG/CR-6974.
[30] Applied Programming Technology Inc, Uncertainty Analysis User's Manual Symbolic Nuclear Analysis Package (SNAP), APT Inc., Bloomsburg, PA, 2021.
[31] J.I. Daoud, Multicollinearity and regression analysis, J. Phys. Conf. Ser. 949 (2018) 1, https://doi.org/10.1088/1742-6596/949/1/012009.
[32] K. Il Ahn, S.H. Park, H.D. Kim, H.S. Park, The plant-specific uncertainty analysis for an ex-vessel steam explosion-induced pressure load using a Texas-SAUNA coupled system, Nucl. Eng. Des. 249 (2012) 400–412, https://doi.org/10.1016/j.nucengdes.2012.04.015.
[33] M. Statistics, Determination of Sample Sizes for Setting Tolerance Limits Author (s): S . S . Wilks Source : The Annals of Mathematical Statistics , Vol . 12 , No . 1 (Mar ., 1941), pp . 91-96 determination of sample sizes for setting tolerance, vol. 12, 2014, pp. 91–96, 1.